Biological Assessment of Manganese Oxide Nanoparticles Synthesized via Green and Chemical Methods Using Turmeric and Lemon Extracts

Nadia Jasim Ghdeeb[1] and Sura Hadi Hussien[2]
[1]*Department of Physics, College of Science, Mustansiriyah University, 10052 Baghdad, Iraq*
[2]*Ministry of Education, 10001 Baghdad, Iraq*
nadiajasim127@uomustansiriyah.edu.iq, surahadi76@yahoo.com

Keywords: MnO_2 NPs, Biosynthesis, Structure, Optical Properties, Antibacterial Activity.

Abstract: The Manganese Dioxide nanoparticles (MnO2 NPs) were synthesised using chemical method, turmeric extract and Lemon extract leaf extracts by green synthesis method. The synthesised nanoparticles were characterized by XRD, FESEM techniques and UV-Vis absorption. XRD analysis confirms that the prepared MnO2 NPs was in orthohombic structure, and the size of MnO2 NPs was estimated in the range of 89.388, 65.947 and 65.924nm for chemical method, turmeric extract and Lemon extract leaf respectively. FESEM images revealed that the particles were spherical in shape. The absorption of all oxides decreases with increasing wavelength for all samples prepared by both the chemical and green methods. Synthesized MnO2 nanoparticles were found to exhibit good antibacterial activity, with MnO2Nps extracted from lemon showing higher antibacterial activity with zone exceeding 20 and 25 mm for Gram-negative bacteria (E. coli and Klebsiella sp.) and 26 and 19 mm for Gram-positive bacteria (S. aureus and S. epidermidis), respectively. than those extracted from turmeric with zone exceeding 15 and 13 mm for Gram-negative bacteria (E. coli and Klebsiella sp.) and 13 and 14 mm for Gram-positive bacteria (S. aureus and S. epidermidis), respectively. and 13 and 13 mm for Gram-negative bacteria (E. coli and Klebsiella sp.) and 10 and 5 mm for Gram-positive bacteria (S. aureus and S. epidermidis), respectively chemically synthesized.

1 INTRODUCTION

Nanotechnology is a young, exciting field that could be used to produce biomedical, household, and industrial goods. There is an increasing risk of nanomaterial exposure to humans and the environment as a result of the growing number of applications. Our understanding of the impacts of manufactured nano-sized contaminants on biological systems is currently lacking, and their potential toxicological effects are actively being investigated. Applications of nanotechnology in medicine and microbiology hold promise for eradicating infectious disease resistance. Researchers have used a variety of antibacterial chemicals, including nanoparticles like metal and metal oxide, to combat different bacteria [1]. Because of their fundamental importance as well as the prospective technical uses, nanomaterials have garnered a lot of interest. Nanoscale materials have different properties than bulk materials in a variety of domains, including catalysis, electrical, and magnetic. Researchers are becoming increasingly interested in nanotechnology due to manganese dioxide's (MnO_2) low toxicity. This means that nanomaterials can be applied to many fields, such as medicine, electronics, and the environment [2]. Recently, due to their unique structures, magnetic behaviours, luminescence properties, and reaction activities, transition metal oxide nanoparticles have garnered scientific attention [3]. Manganese oxide nanoparticles exhibit great potential for use in spintronics and energy storage applications when compared to other transition metal oxides [4], [5]. Further possible uses for manganese oxide nanoparticles include medication delivery [6], biosensors [7], cancer treatment [8], magnetic resonance imaging (MRI) agents [9], and catalysis [8]. There are two possible ways for fabricating MnO_2 NPs: ascending and descending. In order to generate subjects with homogeneous size and shape, most researchers prefer the upward route because of the higher configuration cost and structural faults in the manufactured NPs, from top to bottom. This

approach is not widely used.Numerous crystal formations of MnO_2 are known to exist, such as a-(hollandite), b- (pyrrulozite), c- (sutite), d-(birnessite), k- (akhtensite),With a different bonding, we employ the same basic structure as MnO_2 [10]-[12]. Antibacterial, antimycotic, antibiofilm, and antioxidant applications are among the numerous biological applications for which metal oxides (CuO, MnO, ZnO, NiO, MgO, FeO, Fe_2O_3, Cr_2O_3, etc.) and metals (Au, Ag, Pt, Pd, Mn, Zn, Cu, etc.) nanoparticles (NPs) are extensively researched and utilized [13].

The aim of the research is to prepare manganese oxide by the chemical method and the green method and to compare the physical properties and antibacterial activity.

2 MATERIALS AND METHODS

2.1 Materials

Manganese chloride ($MnCl_3$), turmeric and fresh Lemon from Baghdad, Iraq, were procured from the local market in Iraq. Distilled and deionized water were employed in all experimental procedures.

2.2 Experimental Part

2.2.1 Manganese Oxide Production Method

Manganese chloride ($MnCl_3$) was employed to produce nanoparticles (MnO_2), with a purity of 99.9% and a chemical formula of ($MnCl_3$).

Aqueous manganese chloride was dissolved in 50 ml of deionized water at a concentration of 0.1 M. After filtering and washing the solution multiple times, the sediment is allowed to dry before being burned in an oven at 300 Cº Celsius for two hours. Sodium hydroxide (NaOH) is added to the manganese chloride solution drop by drop and mixed thoroughly with a magnetic stirrer at room temperature. The preparation stages of MnO_2 NPs using chemical method in Figure 1.

2.2.2 Method of Producing Turmeric Extract

Turmeric extract was produced by combining 10 g of curcuma with 100 ml of sterile distilled water. Next, the mixture was heated to a boil for 5 minutes or until the color of the aqueous solution changed to yellow. After that, the mixture was centrifuged for 5 minutes at 2000 rpm, filtered through filter paper, then leave it to cool until it reaches room temperature to eliminate the biomaterials. Figure 2 the preparation stages of MnO_2 NPs using turmeric extract.

2.2.3 Lemon Extract Production Method

50 ml of filtered lemon juice was prepared at room temperature. To produce manganese oxide nanoparticles, add 10 ml of manganese chloride solution to 10 ml of lemon juice. The mixture was stirred continuously for one hour at room temperature for 15 minutes, resulting in a pale-yellow solution. The precipitates were then heated in an oven at 300°C for 2 hours. Figure 1 shows that process steps for preparing MnO_2 NPs using the green method.

Figure 1: Process steps for preparing MnO_2 NPs using chemical method.

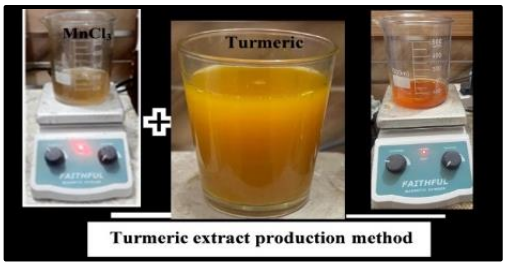

Figure 2: Process steps for preparing MnO_2 NPs using turmeric extract.

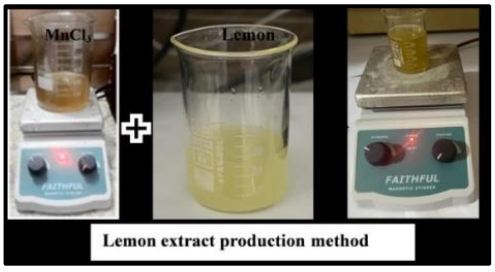

Figure 3: Process steps for preparing MnO2 NPs using Lemon extract.

The extract was kept at room temperature. The preperation manganese oxide nanoparticles 10 ml of

aqueous manganese chloride solution added to 10 ml of the aqueous yellow turmeric extract.

The precipitates were then heated in an oven at 300 °C for 2 hours. Figure 3 Process steps for preparing MnO_2 NPs using Lemon extract.

3 RESULTS AND DISCUSSION

3.1 XRD of MnO_2 Nanoparticles

Figure 4 illustrates XRD patern of MnO_2 nanopowder synthesized at room temperature using the chemical and green method (Lemon extract and turmeric extract). The crystal structure and orientation of manganese oxide nanoparticles were determined using an XRD pattern. The corresponding planes are identified by utilizing the 2θ values (27.498, 35.121, 43.848, 50.613, 59.810, 64.828 and 77.772), for the following peak positions: (201), (301), (401), (410), (600), (203), (213), and in the preferential direction, (301). The values obtained are in agreement with the powder MnO_2 data card from the International Center for Diffraction (JCPDS-44-0142). In the absence of supplementary diffraction peaks the low degree of crystallinity is the reason for the small peak intensities of MnO_2. According to the Debye–Scherrer (1) the average crystallite size of the MnO_2 nanosheets produced by the chemical method and the green method (Lemon extract and turmeric extract) was 89.388 nm and 65.947, 65.924, respectively. Table 1 show the structural parameters of MnO_2 NPs.

$$D=0.9\lambda/\beta cos\theta. \quad (1)$$

3.2 Field Emission Scanning Electron Microscopy (FE-SEM) analysis

The surface morphology of MnO_2 nanoparticles and the particle size was determined using the scanning electron microscope (SEM). Figure 5 depict SEM images of MnO_2 NPs. The agglomeration exhibited spherical morphologies, and the particle size of MnO_2 NPs was well disseminated, ranging between (48.77-87.57) nm.

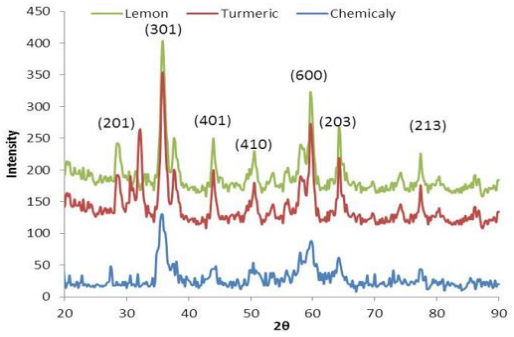

Figure 4: XRD patern of MnO_2 NPs.

Table 1: The structural parameters of MnO_2 NPs.

	2θ stand (deg.)	2 θ Exp. (deg.)	FWHM (rad)	Millerindices (h k l)	D(nm)	D av.(nm)
Chemical Method	27.49	28.65	0,03254	(201)	45,7666	89.38
	35.12	35.85	0,03159	(301)	47,1437	
	43.84	44.01	0,01709	(401)	87,1293	
	50.61	50.47	0,01519	(410)	98,0217	
	59.81	59.68	0,01901	(600)	78,3364	
	64.82	64.25	0,01738	(203)	85,6694	
	77.77	77.36	0.01677	(313)	88,7780	
Turmeric extract	27.49	27.41	0.02703	(201)	52.6770	65.94
	35.12	35.71	0.02479	(301)	58.4692	
	43.84	43.96	0.02326	(401)	64.0049	
	50.61	50.62	0.02911	(410)	52.8024	
	59.81	59.62	0.02410	(600)	66.0625	
	64.82	64.12	0.02195	(203)	74.0823	
	77.77	77.39	0.01895	(313)	93.3552	
Lemon extract	27.49	27.55	0.02710	(201)	52.678	65.92
	35.12	35.75	0.02491	(301)	58.469	
	43.84	43.82	0.02335	(401)	64.004	
	50.61	50.80	0.02907	(410)	52.802	
	59.81	59.81	0.02421	(600)	66.063	
	64.82	64.26	0.02210	(203)	74.083	
	77.77	77.52	0.01904	(313)	93.369	

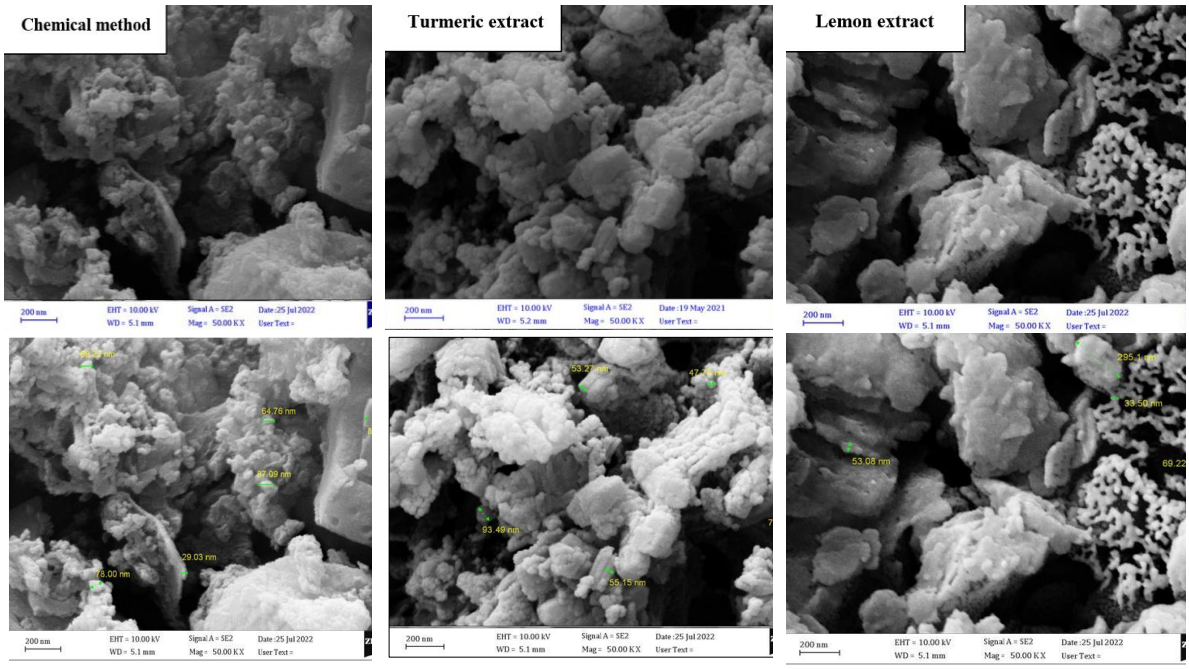

Figure 5: FE-SEM images of MnO_2 NPs.

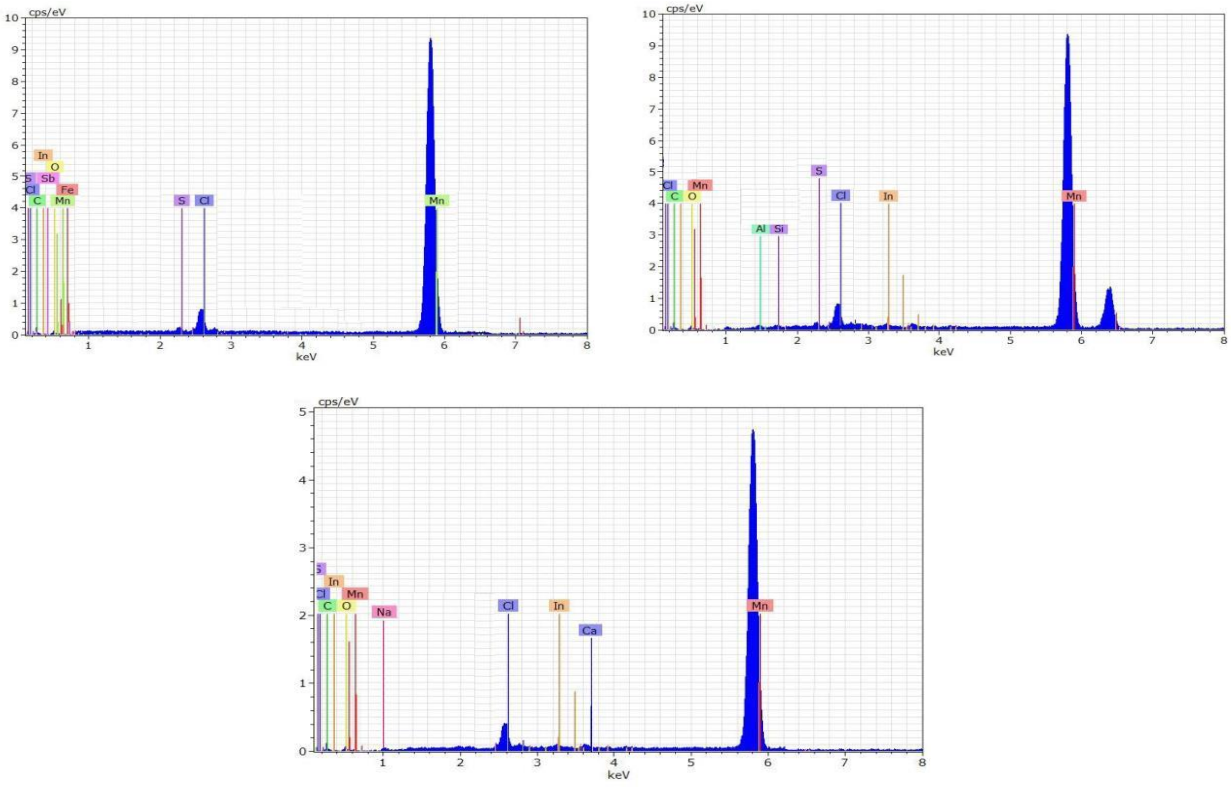

Figure 6: The EDX pattern of of MnO2 nanostructure.

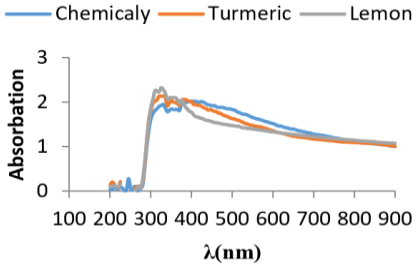

Figure 7: Optical absorbance spectrum of MnO_2 Nanoparticles.

Energy dispersive X-ray analysis is advantageous for determining the elemental composition of a chemical. It was utilized in this work to demonstrate the proportions of elements in chemically and green synthesized oxides. The energy dispersive X-ray (EDX) profile confirmed the Mn and O signaling property. Energy dispersive X-ray analysis of MnO_2 Nps is shown in Figure 6.

3.3 Optical Absorption Spectrum

The optical characteristics of MnO_2 NPs were evaluated using absorbance (A) measurements in the 200–900 nm range. The absorbance spectra of MnO_2 NPs are shown in Figure 7. The absorption of all oxides decreases with increasing wavelength, and magnesium oxide prepared using lemon has the highest absorbance compared to magnesium oxide prepared using turmeric and the chemical method, as shown in the Figure 7. This means that the photon does not have enough energy to interact with the material's atoms and thus cannot irritate the electron and transfer it from the valence band to the conduction band. Because the incident photon's energy is less than the value of the energy gap, the absorbance decreases with increasing wavelength due to the inverse relationship between wavelength and photon energy [14].

4 ANTIMICROBIAL ACTIVITY EVALUATION

This section must be in two columns. Each The antibacterial activity of produced MnO_2 NPs, was evaluated utilizing a range of harmful bacteria, including Gram positive (S. aureus and St. epidermidis) and Gram-negative bacteria (E. coli and Klebsiella sp.).

Inhibition zones (13,15,10mm) and (13,13,25 mm) of gram-negative bacteria E. coli and Klebsiella sp., respectively.

Meanwhile, the inhibition zones of MnO_2 Nps for Gram-positive bacteria S. aureus and S. epidermidis were (10, 13, 26 mm) and (10, 14,19 mm), respectively (Fig. 8).

The green method using lemon was clearly effective for all bacterial species, with zone exceeding 20 and 25 mm for Gram-negative bacteria (E. coli and Klebsiella sp.) and 26 and 19 mm for Gram-positive bacteria (S. aureus and S. epidermidis), respectively. These results indicate that the green method, particularly the use of lemon extract, significantly enhanced the bioactivity of manganese oxide nanoparticles. This may be explained by the presence of bioactive compounds in plant extracts, such as flavonoids, polyphenols, and citric acid, which act as reducing agents. These properties increase the ability of the particles to adhere to and destroy the bacterial cell membrane by generating reactive oxygen species (ROS) or inhibiting vital cellular enzymes. Table 2 inhibition zone of the MnO_2 NPs activity towards selected pathogenic bacteria.

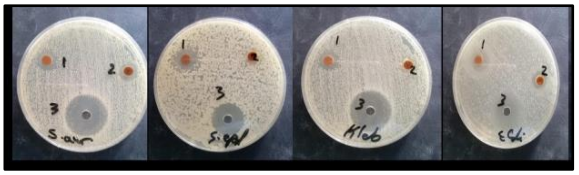

Figure 8: Activity of MnO_2 NPs towards selected pathogenic bacteria.

Table 2: Inhibition zone of the MnO_2 NPs activity towards selected pathogenic bacteria.

Type bacterial	Organisms	Inhibition zone (mm)		
		Chemial Method	Green Method	
Gram - Negative		(2)	Turmeric (1)	Lemon (3)
	E. coli	13	15	20
	Klebsiella sp	13	13	25
Gram - Positive	S. aureus	10	13	26
	st. epidermidis	5	14	19

5 CONCLUSIONS

MnO_2 nanoparticles were successfully synthesized via chemical and green routes (turmeric and lemon extracts), enabling a comparative evaluation of

synthesis-dependent properties. XRD confirmed orthorhombic phase formation in all samples, with reduced crystallite size in green-synthesized nanoparticles (≈65.92–65.94 nm) compared to chemically synthesized material (≈89.38 nm), indicating phytochemical-mediated growth inhibition. FESEM revealed predominantly spherical morphology with nanoscale aggregation, while EDX verified elemental purity.

UV–Vis analysis demonstrated wavelength-dependent absorbance behavior, with lemon-derived MnO_2 exhibiting enhanced optical response relative to other samples. Antibacterial assessment showed significant activity against both Gram-positive and Gram-negative strains, with green-synthesized nanoparticles—particularly lemon-based—exhibiting superior inhibition zones. The improved bioactivity is attributed to reduced particle size, increased surface reactivity, and phytochemical-assisted ROS generation.

Overall, green synthesis provided a more efficient and functionally enhanced route for MnO_2 nanoparticle production compared to the chemical method. The obtained nanoparticles demonstrate strong potential for antimicrobial applications. Further studies are required to evaluate cytotoxicity, stability, and in vivo performance.

REFERENCES

[1] A. H. Ghdeeb, N. Jasim, A. M. Abdulmajeed, and M. Mohammed, "Role of Extracted Nano-Metal Oxides from Factory Wastes in Medical Applications," Iraqi Journal of Science, vol. 64, 2023.

[2] C. Burda, X. B. Chen, R. Narayanan, and M. A. El-Sayed, "Chemistry and Properties of Nanocrystals of Different Shapes," Chemical Reviews, vol. 105, pp. 1025-1102, 2005, [Online]. Available: https://doi.org/10.1021/cr030063a.

[3] S. M. Dizaj, S. Jafari, and K. Khezri, "Antimicrobial Activity of Carbon-Based Nanoparticles," Journal of Toxicology, vol. 4, 2013.

[4] V. Ilyasov, B. Meshi, A. Ryzhkin, I. Ershov, and N. I. Ilyasov, "Materials for Spintronics: Magnetic and Transport Properties of Ultrathin (Monolayer Graphene)/MnO(001) and MnO(001) Films," Journal of Modern Physics, 2011, [Online]. Available: https://doi.org/10.4236/jmp.2011.210139.

[5] P. P. Liu, L. Y. Yang, W. Liu, Y. Zhang, H. L. Wang, S. Liu, and R. R. Yang, "Novel Hybrid Anode of MnO Nanoparticles and Ultrathin Carbon Sheets for High Lithium Storage Performance," Journal of Alloys and Compounds, 2018, [Online]. Available: https://doi.org/10.1016/j.jallcom.2017.12.076.

[6] J. Shin, R. M. Anisur, M. K. Ko, G. H. Im, and I. S. Lee, "Hollow Manganese Oxide Nanoparticles as Multifunctional Agents for Magnetic Resonance Imaging and Drug Delivery," Angewandte Chemie International Edition, 2009, [Online]. Available: https://doi.org/10.1002/anie.200802323.

[7] J. J. Xu, W. Zhao, X. L. Luo, and H. Y. Chen, "A Sensitive Biosensor for Lactate Based on Layer-by-Layer Assembling MnO_2 Nanoparticles and Lactate Oxidase on Ion-Sensitive Field-Effect Transistors," Chemical Communications, 2005, [Online]. Available: https://doi.org/10.1039/B416548A.

[8] O. Jankovský, D. Sedmidubský, P. Šimek, Z. Sofer, and U. Pumera, "Synthesis of MnO, Mn_2O_3 and Mn_3O_4 Nanocrystal Clusters by Thermal Decomposition of Manganese Glycerolate," Ceramics International, 2014, [Online]. Available: https://doi.org/10.1016/j.ceramint.2014.08.108.

[9] T. D. Schladt, K. Schneider, M. I. Shukoor, F. Natalio, H. Bauer, M. N. Tahir, S. Weber, and L. M. Schreiber, "Highly Soluble Multifunctional MnO Nanoparticles for Simultaneous Optical and MRI Imaging and Cancer Treatment Using Photodynamic Therapy," Journal of Materials Chemistry, 2010, [Online]. Available: https://doi.org/10.1021/nn501652j.

[10] M. M. Najafpour and S. I. Allakhverdiev, "Manganese Compounds as Water Oxidizing Catalysts for Hydrogen Production via Water Splitting: From Manganese Complexes to Nano-Sized Manganese Oxides," International Journal of Hydrogen Energy, 2012, [Online]. Available: https://doi.org/10.1016/j.ijhydene.2012.02.075.

[11] T. Lin, L. Yu, M. Sun, et al., "Mesoporous α-MnO_2 Microspheres with High Specific Surface Area: Controlled Synthesis and Catalytic Activities," Chemical Engineering Journal, 2016, [Online]. Available: https://doi.org/10.1016/j.cej.2015.09.024.

[12] V. Štengl, D. Králová, F. Opluštil, et al., "Mesoporous Manganese Oxide for Warfare Agents Degradation," Microporous and Mesoporous Materials, 2012, [Online]. Available: https://doi.org/10.1016/j.micromeso.2012.02.031.

[13] H. Lu, X. Zhang, S. A. Khan, and W. Li, "Biogenic Synthesis of MnO_2 Nanoparticles with Leaf Extract of Viola betonicifolia for Enhanced Antioxidant, Antimicrobial, Cytotoxic, and Biocompatible Applications," Frontiers in Microbiology, 2021, [Online]. Available: https://doi.org/10.3389/fmicb.2021.761084.

[14] D. Philip, "Synthesis and Spectroscopic Characterization of Gold Nanoparticles," Spectrochimica Acta Part A: Molecular and Biomolecular Spectroscopy, 2008, [Online]. Available: https://doi.org/10.1016/j.saa.2007.11.012.